CLASSICAL THEORY OF NON-DEGENERATE SUM-FREQUENCY GENERATION BY INCOHERENT NONLINEAR OPTICAL MIXING OF COHERENT AND CHAOTIC RADIATIONS

II. COHERENT AND CHAOTIC INPUT RADIATIONS – EFFICIENCY AND SPECTRAL DISTRIBUTION*)

P. Chmela

Department of Physics, Faculty of Mechanical Engineering, Technical University Brno, Technická 2, 616 69 Brno, Czechoslovakia

Z. Ficek, S. Kielich

Nonlinear Optics Division, Institute of Physics, Adam Mickiewicz University, Grunwaldzka 6, 60—780 Poznań, Poland

Sum-frequency generation by incoherent nonlinear optical mixing of one coherent and one chaotic, mutually uncorrelated input radiations in a dispersive medium is treated in this paper. The efficiency of the process is calculated in the second approximation of the iterative method. It is shown that for perfect phase matching or small phase mismatch of interacting waves and small spectral width of chaotic input radiation the efficiency of incoherent sum-frequency generation can be enhanced compared with the coherent interaction due to the difference between group velocities of sub-frequency radiations. On the other hand, for greater spectral width the efficiency of the process decreases with increasing spectral width of chaotic input radiation. In the case of considerable phase mismatch the efficiency of sum-frequency generation first decreases, but then increases with increasing spectral width of chaotic input radiation. The spectral distribution of the resulting sum-frequency radiation is calculated in the first approximation of the iterative method. There is a general tendency to narrowing the spectral distribution of generated radiation in the course of the process. Moreover, when there is phase mismatch present, a spectral shift of the maximum of generated radiation towards blue or red region, according to the signs of the phase mismatch and the typical dispersion coefficient, appears in the later phases of the sum-frequency generation.

1. INTRODUCTION

In the first part of this investigation [1] we introduced the general classical solution for non-degenerate sum-frequency generation by incoherent nonlinear optical mixing of one coherent and the other chaotic sub-frequency input radiations; both sub-frequency generating radiations were assumed to be mutually uncorrelated at the beginning of the process. The second-step approximation of the iterative method was used when calculating the efficiency of the process and the first-step iterative solution was used for the description of spectral distribution of generated sum-frequency radiation.

In this part we shall deal particularly with the dependence of the efficiency of sum-frequency generation and the spectral distribution of generated radiation upon the

*) This work was partially supported by Research Project C.P.B.P. 01. 07.

coherence and statistical properties of the chaotic sub-frequency input radiation and the characteristic coefficients of the nonlinear medium.

As the efficiency of the process depends upon four parameters [1], we have to make certain simplifications and special cases must be considered in the next treatment.

Concerning the spectral distribution of generated sum-frequency radiation, its form is relatively simple so that we can discuss it more generally.

2. DEFINITIONS AND CALCULATIONS OF INTEGRALS

For further use we define and calculate the following integrals.

(II.1)
$$\mathscr{I}(\eta, \Delta, \tau) = \int_0^\tau \mathrm{d}x_1 \int_0^\tau \mathrm{d}x_2 \exp\left[-\mathrm{i}\Delta(x_1 - x_2) - \eta|x_1 - x_2|\right] =$$
$$= \frac{2\eta}{(\eta^2 + \Delta^2)}\,\tau + \frac{2}{(\eta^2 + \Delta^2)^2}\left[(\eta^2 - \Delta^2)\cos(\Delta\tau) - 2\eta\Delta\sin(\Delta\tau)\right]\exp(-\eta\tau) - \frac{2(\eta^2 - \Delta^2)}{(\eta^2 + \Delta^2)^2},$$

(II.2)
$$\mathscr{E}_1^{(\mathrm{c,ch})}(\eta, \Delta, \tau) =$$
$$= 2\int_0^\tau \mathrm{d}x_1 \int_0^\tau \mathrm{d}x_2 \int_0^{x_2} \mathrm{d}x_2' \int_0^{x_2'} \mathrm{d}x_2'' \cos\left[\Delta(x_1 - x_2 + x_2' - x_2'')\right] \times \exp(-\eta|x_1 - x_2 + x_2' - x_2''|) =$$
$$= \frac{2\eta}{3(\eta^2 + \Delta^2)}\,\tau^3 - \frac{4}{(\eta^2 + \Delta^2)^3}\{\eta(\eta^2 - 3\Delta^2)\left[1 + \cos(\Delta\tau)\exp(-\eta\tau)\right] - \Delta(3\eta^2 - \Delta^2)\sin(\Delta\tau)\exp(-\eta\tau)\}\,\tau + \frac{8}{(\eta^2 + \Delta^2)^4}\{(\eta^4 - 6\eta^2\Delta^2 + \Delta^4) \times \left[1 - \cos(\Delta\tau)\exp(-\eta\tau)\right] + 4\eta\Delta(\eta^2 - \Delta^2)\sin(\Delta\tau)\exp(-\eta\tau)\},$$

(II.3)
$$\mathscr{E}_2^{(\mathrm{c,ch})}(\eta, \Delta, \tau) =$$
$$= 2\int_0^\tau \mathrm{d}x_1 \int_0^\tau \mathrm{d}x_2 \int_0^{x_2} \mathrm{d}x_2' \int_0^{x_2'} \mathrm{d}x_2'' \cos\left[\Delta(x_1 - x_2 + x_2' - x_2'')\right] \times \exp\left[-\eta(|x_1 - x_2| + x_2' - x_2'')\right] =$$
$$= 2\int_0^\tau \mathrm{d}x_1 \int_0^\tau \mathrm{d}x_2 \int_0^{x_2} \mathrm{d}x_2' \int_0^{x_2'} \mathrm{d}x_2'' \cos\left[\Delta(x_1 - x_2 + x_2' - x_2'')\right] \times \exp\left[-\eta(|x_1 - x_2''| + x_2 - x_2')\right| =$$
$$= \frac{2\eta^2}{(\eta^2 + \Delta^2)^2}\,\tau^2 - \frac{2}{(\eta^2 + \Delta^2)^3}\{\eta(3\eta^2 - 5\Delta^2) - 2\Delta\left[2\eta\Delta\cos(\Delta\tau) + (\eta^2 - \Delta^2)\sin(\Delta\tau)\right]\exp(-\eta\tau)\}\,\tau + \frac{1}{(\eta^2 + \Delta^2)^4}\{7\eta^4 - 34\eta^2\Delta^2 + 7\Delta^4 + (\eta^2 + \Delta^2)^2\exp(-2\eta\tau)$$

$$- 8[(\eta^4 - 4\eta^2\Delta^2 + \Delta^4)\cos(\Delta\tau) - 3\eta\Delta(\eta^2 - \Delta^2)\sin(\Delta\tau)]\exp(-\eta\tau)\}\,,$$

(II.4)

$$\mathscr{F}_1^{(c,ch)}(\eta, \Delta, \tau) =$$

$$= 2\int_0^\tau dx_1 \int_0^\tau dx_2 \int_0^{x_2} dx_2' \int_0^{x_2'} dx_2'' \cos[\Delta(x_1 - x_2 + x_2' - x_2'')]$$

$$\times \exp[-\eta(|x_1 + x_2 - x_2' - x_2''| + 2x_2 - 2x_2')] =$$

$$= \frac{\eta^2}{(\eta^2 + \Delta^2)^2}\tau^2 - \frac{\eta(3\eta^2 - 7\Delta^2)}{(\eta^2 + \Delta^2)^3}\tau - \frac{4}{(\eta^2 + \Delta^2)^3(9\eta^2 + \Delta^2)}$$

$$\times [\eta(3\eta^4 - 14\eta^2\Delta^2 - \Delta^4)\cos(\Delta\tau) - \Delta(11\eta^4 - 6\eta^2\Delta^2 - \Delta^4)\sin(\Delta\tau)]\,\tau\exp(-\eta\tau)$$

$$+ \frac{1}{(\eta^2 + \Delta^2)}\left\{\left[\frac{(\eta^2 - 3\Delta^2)}{2(\eta^2 + \Delta^2)^2} - \frac{4(\eta^4 - 6\eta^2\Delta^2 + \Delta^4)}{(\eta^2 + \Delta^2)^3} - \frac{(9\eta^2 + 5\Delta^2)}{2(9\eta^2 + \Delta^2)^2}\right]\cos(\Delta\tau)\right.$$

$$\left. - \Delta\left[\frac{(3\eta^2 - \Delta^2)}{2\eta(\eta^2 + \Delta^2)^2} - \frac{16\eta(\eta^2 - \Delta^2)}{(\eta^2 + \Delta^2)^3} - \frac{(3\eta^2 - \Delta)^2}{2\eta(9\eta^2 + \Delta^2)^2}\right]\sin(\Delta\tau)\right\}\exp(-\eta\tau)$$

$$- \frac{\eta}{2(\eta^2 + \Delta^2)^4}[\eta(\eta^2 - 4\Delta^2)\cos(2\Delta\tau) - \Delta(3\eta^2 - \Delta^2)\sin(2\Delta\tau)]\exp(-2\eta\tau)$$

$$+ \frac{(9\eta^2 - 5\Delta^2)}{2(\eta^2 + \Delta^2)(9\eta^2 + \Delta^2)^2}\exp(-4\eta\tau) - \frac{(\eta^2 - 5\Delta)^2}{4(\eta^2 + \Delta^2)^3} + \frac{17(\eta^4 - 6\eta^2\Delta^2 + \Delta^4)}{4(\eta^2 + \Delta^2)^4}\,,$$

(II.5)

$$\mathscr{F}_2^{(c,ch)}(\eta, \Delta, \tau) =$$

$$= \lim_{|\varkappa|\to\infty} 2\int_0^\tau dx_1 \int_0^\tau dx_2 \int_0^{x_2} dx_2' \int_0^{x_2'} dx_2'' \cos[\Delta(x_1 - x_2 + x_2' - x_2'')]$$

$$\times \exp\{-\eta[|\varkappa|(x_2 - x_2') + |x_1 - (1 - \varkappa)(x_2 - x_2') - x_2''|]\} =$$

$$= -\frac{2\eta(\eta^2 - 3\Delta^2)}{(\eta^2 + \Delta^2)^3}\tau - \frac{2}{(\eta^2 + \Delta^2)^3}[\eta(\eta^2 - 3\Delta^2)\cos(\Delta\tau) - \Delta(3\eta^2 - \Delta^2)\sin(\Delta\tau)]$$

$$\times \tau\exp(-\eta\tau) - \frac{4}{(\eta^2 + \Delta^2)^4}[(\eta^4 - 6\eta^2\Delta^2 + \Delta^4)\cos(\Delta\tau) - 4\eta\Delta(\eta^2 - \Delta^2)\sin(\Delta\tau)]$$

$$\times \exp(-\eta\tau) + \frac{4(\eta^4 - 6\eta^2\Delta^2 + \Delta^4)}{(\eta^2 + \Delta^2)^4}\,.$$

3. EFFICIENCY OF THE PROCESS

The second approximation iterative solution for the mean photon flux of sum-frequency radiation at $\omega_3 = \omega_1 + \omega_2$ generated by the incoherent nonlinear optical mixing of one coherent (ω_1) and the other chaotic (ω_2) sub-frequency input radiations has been found to be (see equations (I.25) in [1])

(II.6)

$$\langle N_3(\tau)\rangle_{\mathrm{coh\,chaot}} = \langle N_{1,0}\rangle^{1/2}\langle N_{2,0}\rangle^{1/2}\mathscr{I}(\eta_2, \Delta, \tau) -$$

$$- \langle N_{1,0}\rangle\,\mathscr{E}_1^{(c,ch)}(\eta_2, \Delta, \tau) - \langle N_{2,0}\rangle\,[\mathscr{E}_2^{(c,ch)}(\eta_2, \Delta, \tau) + \mathscr{F}_0^{(c,ch)}(\eta_2, \varkappa_2, \Delta, \tau)]\,.$$

The following notation has been used (see [1]): $\langle N_{1,0}\rangle$, $\langle N_{2,0}\rangle$ are the mean photon fluxes of sub-frequency input radiations, $\tau = \langle N_{1,0}\rangle^{1/4} \langle N_{2,0}\rangle^{1/4} \mu z$ is the reduced normal distance from the first boundary of nonlinear medium, $\Delta = \Delta k/\langle N_{1,0}\rangle^{1/4} . \langle N_{2,0}\rangle^{1/4} \mu$ is the reduced phase mismatch, μ denotes the nonlinear coupling constant, $\eta_2 = \Gamma_{2,0}|\varepsilon_{23}|/\langle N_{1,0}\rangle^{1/4} \langle N_{2,0}\rangle^{1/4} \mu$ is the reduced spectral half width of the chaotic sub-frequency input radiation, $\varepsilon_{jk} = (1/u_{rgk} - \cos \alpha_{jk}/u_{rgj})/\cos \beta_k$ being the typical dispersion coefficients, u_{rgj} are group velocities in ray directions, α_{jk} are the divergence angles between two ray directions $\mathbf{f}_j$ and $\mathbf{f}_k$, β_j are refractive angles of the ray directions and $\varkappa_2 = \varepsilon_{21}/\varepsilon_{23}$. The functions $\mathscr{I}(\eta_2, \Delta, \tau)$, $\mathscr{E}_1^{(c,ch)} . (\eta_2, \Delta, \tau)$ and $\mathscr{E}_2^{(c,ch)}(\eta_2, \Delta, \tau)$ are given by equations (II.1), (II.2) and (II.3), respectively, and

(II.7)
$$\mathscr{F}_0^{(c,ch)}(\eta_2, \varkappa_2, \Delta, \tau) = = 2 \int_0^\tau dx_1 \int_0^\tau dx_2 \int_0^{x_2} dx_2' \int_0^{x_2'} dx_2'' \cos [\Delta(x_1 - x_2 + x_2' - x_2'')] \times \exp \{-\eta_2[|\varkappa_2| (x_2 - x_2') + |x_1 - (1 - \varkappa_2)(x_2 - x_2') - x_2''|]\},$$

the explicit calculation of $\mathscr{F}_0^{(c,ch)}(\eta_2, \varkappa_2, \Delta, \tau)$ being given by equations (I.29) in [1].

For perfect phase matching of interacting waves, if $\Delta = 0$, equation (II.6) is reduced to simpler forms:

for $\varkappa_2 > 0$

(II.6a′)
$$\langle N_3(\tau)\rangle_{\text{coh chaot}} = \frac{2\langle N_{1,0}\rangle^{1/2} \langle N_{2,0}\rangle^{1/2}}{\eta_2} \left\{\tau - \frac{1}{\eta_2}[1 - \exp(-\eta_2\tau)]\right\} - \frac{2\langle N_{1,0}\rangle}{\eta_2} \left\{\frac{\tau^3}{3} - \frac{2\tau}{\eta_2^2}[1 + \exp(-\eta_2\tau)] + \frac{4}{\eta_2^3}[1 - \exp(-\eta_2\tau)]\right\} - \frac{\langle N_{2,0}\rangle}{\eta_2^2} \left\{\frac{2(1 + \varkappa_2)}{\varkappa_2}\tau^2 - \frac{4(1 + 2\varkappa_2^2)}{\varkappa_2^2\eta_2}\tau - \frac{4(1 - \varkappa_2)}{\eta_2(1 - 2\varkappa_2)}\tau \exp(-\eta_2\tau) - \frac{4(12\varkappa_2^2 - 13\varkappa_2 + 4)}{\eta_2^2(1 - 2\varkappa_2)^2} \exp(-\eta_2\tau) + \frac{\exp(-2\eta_2\tau)}{\eta_2^2} - \frac{4\exp(-\varkappa_2\eta_2\tau)}{\varkappa_2^3\eta_2^2} + \frac{\exp(-2\varkappa_2\eta_2\tau)}{\varkappa_2\eta_2^2(1 - 2\varkappa_2)^2} + \frac{(11\varkappa_2^3 - \varkappa_2^2 + 4)}{\varkappa_2^3\eta_2^2}\right\},$$

for $\varkappa_2 < 0$

(II. 6a″)
$$\langle N_3(\tau)\rangle_{\text{coh chaot}} = \frac{2\langle N_{1,0}\rangle^{1/2} \langle N_{2,0}\rangle^{1/2}}{\eta_2} \left\{\tau - \frac{1}{\eta_2}[1 - \exp(-\eta_2\tau)]\right\} - \frac{2\langle N_{1,0}\rangle}{\eta_2} \left\{\frac{\tau^3}{3} - \frac{2\tau}{\eta_2^2}[1 + \exp(-\eta_2\tau)] + \frac{4}{\eta_2^3}[1 - \exp(-\eta_2\tau)]\right\} - \frac{\langle N_{2,0}\rangle}{\eta_2^2} \left\{\frac{2(1 + |\varkappa_2|)}{|\varkappa_2|}\tau^2 - \frac{2(8|\varkappa_2|^3 + 5\varkappa_2^2 + 4|\varkappa_2| + 2)}{\varkappa_2^2\eta_2(1 + 2|\varkappa_2|)}\tau - \frac{2}{\eta_2}\tau \exp(-\eta_2\tau)\right.$$

$$- \frac{(12|\varkappa_2| + 1)}{|\varkappa_2| \eta_2^2} \exp(-\eta_2 \tau) + \frac{\exp(-2\eta_2\tau)}{\eta_2^2} - \frac{4 \exp(-|\varkappa_2| \eta_2 \tau)}{|\varkappa_2|^3 \eta_2^2}$$

$$+ \frac{\exp[-(1 + 2|\varkappa_2|) \eta_2 \tau]}{|\varkappa_2| \eta_2^2 (1 + 2|\varkappa_2|)^2} + \frac{4(1 + 3|\varkappa_2|^3)}{|\varkappa_2|^3 \eta_2^2} + \frac{(3 - 4\varkappa_2^2)}{\eta_2^2(1 + 2|\varkappa_2|)^2} \Big\} .$$

The numerical calculations of (II.6a) have shown that for great absolute values $\varkappa_2, |\varkappa_2| \gg 1$, and small $\eta_2, \eta_2 \lessapprox 1$, the dependence of efficiency of sum-frequency generation upon $|\varkappa_2|$ is practically the same for both positive and negative $\varkappa_2$.

For small spectral width of the chaotic input radiation or small group velocity dispersion, or for the beginning of the process, if $\eta_2 \tau \ll 1$, equation (II.6) is simplified as follows:

(II.6b)
$$\langle N_3(\tau) \rangle_{\text{coh chaot}} = \frac{4\langle N_{1,0}\rangle^{1/2} \langle N_{2,0}\rangle^{1/2}}{\Delta^2} \sin^2(\Delta\tau/2)$$

$$- (\langle N_{1,0}\rangle + 2\langle N_{2,0}\rangle) \frac{4}{\Delta^2} \left[\frac{4}{\Delta^2} \sin^2(\Delta\tau/2) - \frac{\tau}{\Delta} \sin(\Delta\tau) \right].$$

In order to determine realistically the values of $\varkappa_2$ for numerical calculations, we shall consider two types of nonlinear interaction, for which the phase matching in an anisotropic medium is possible, namely $\gamma_{\omega_1}^{(II)} + \gamma_{\omega_2}^{(II)} \to \gamma_{\omega_3}^{(I)}$ and $\gamma_{\omega_1}^{(I)} + \gamma_{\omega_2}^{(II)} \to \gamma_{\omega_3}^{(I)}$ or $\gamma_{\omega_1}^{(II)} + \gamma_{\omega_2}^{(I)} \to \gamma_{\omega_3}^{(I)}$ [2–4]. By I and II two polarization modes of light are denoted that correspond to certain wave propagation direction $\mathbf{s}_j$ in the anisotropic medium, provided it holds for corresponding indices of refraction that $n_{\omega_j}^{(I)}(\mathbf{s}_j) \leqq n_{\omega_j}^{(II)}(\mathbf{s}_j)$ (see e.g. [5]). Considering the almost transparent frequency region of the nonlinear medium, in which the group velocities of interaction waves do not differ much from the phase velocities [6], we can roughly estimate the values of $\varkappa_2$ for different ratios of sub-frequencies: $\omega_1 \approx \omega_2$ and $\omega_1 \gg \omega_2$ or $\omega_1 \ll \omega_2$, and different types of nonlinear interaction. The efficiency of the process will then be computed for perfect phase matching ($\Delta = 0$) and great phase mismatch ($|\Delta| = 10$), and for various values of η_2. As the reduced spectral half width η_2 involves the typical dispersion coefficient ε_{23} and also the reduced phase mismatch Δ is not independent of $\varkappa_2$, this procedure can represent a rough approach to the real cases only. An exact description would be possible barely for concrete nonlinear materials.

In the next treatise we introduce the expressions for mean photon fluxes $\langle N_3(\tau)\rangle$ in some special cases corresponding to general expression (II.6) for different values of $\varkappa_2$. The used functions $\mathscr{I}(\eta, \Delta, \tau)$, $\mathscr{E}_1^{(c,ch)}(\eta, \Delta, \tau)$, $\mathscr{E}_2^{(c,ch)}((\eta, \Delta, \tau)$, $\mathscr{F}_1^{(c,ch)}(\eta, \Delta, \tau)$ and $\mathscr{F}_2^{(c,ch)}(\eta, \Delta, \tau)$ are defined by equations (II.1) – (II.5), respectively. As to the computations of the efficiency of sum-frequency generation, we assume that the mean photon fluxes of input radiations are equal: $\langle N_{1,0}\rangle = \langle N_{2,0}\rangle = \langle N_0\rangle$.

Note that a special case of incoherent sum-frequency generation with one strong coherent pump and the other weak chaotic input radiation (parametric up-conversion) was considered in [7].

In order to get an opinion about the accuracy of the used approximation we also introduce the evolution of relative mean photon flux $\langle N_3(\tau)\rangle_{\text{coh chaot}}/\langle N_0\rangle$ that corresponds to the closed solution of coherent sum-frequency generation ($\Delta = 0$, $\eta_2 = 0$) [8] in those figures that represent the evolution of relative mean photon fluxes in the phase matched ($\Delta = 0$) process.

The following special cases are considered.

1. $\omega_1 \approx \omega_2$.

a) Type of interaction: $\gamma_{\omega_1}^{(\mathrm{II})} + \gamma_{\omega_2}^{(\mathrm{II})} \to \gamma_{\omega_3}^{(\mathrm{I})}$, $|\varkappa_2| \ll 1$.

(II.8)
$$\langle N_3(\tau)\rangle_{\text{coh chaot}} = \langle N_{1,0}\rangle^{1/2} \langle N_{2,0}\rangle^{1/2} \mathscr{I}(\eta_2, \Delta, \tau) -$$
$$- \langle N_{1,0}\rangle \mathscr{E}_1^{(\text{c,ch})}(\eta_2, \Delta, \tau) - \langle N_{2,0}\rangle \left[\mathscr{E}_1^{(\text{c,ch})}(\eta_2, \Delta, \tau) + \mathscr{E}_2^{(\text{c,ch})}(\eta_2, \Delta, \tau)\right].$$

The evolution of relative mean photon flux $\langle N_3(\tau)\rangle_{\text{coh chaot}}/\langle N_0\rangle$ ($\langle N_0\rangle = \langle N_{1,0}\rangle = \langle N_{2,0}\rangle$) in the course of incoherent sum-frequency generation for perfect phase matching ($\Delta = 0$) and great phase mismatch ($|\Delta| = 10$) and for various values of η_2 is shown in fig. 1 in this case. It follows that for perfect phase matching (or for small values of $|\Delta|$) the efficiency of the process decreases with increasing coefficient η_2 (with increasing spectral half width $\Gamma_{2,0}$ and with increasing absolute value of typical dispersion coefficient $|\varepsilon_{23}|$) (see fig. 1a). However, for great phase mismatch a reverse effect occurs, namely, the efficiency of sum-frequency generation first

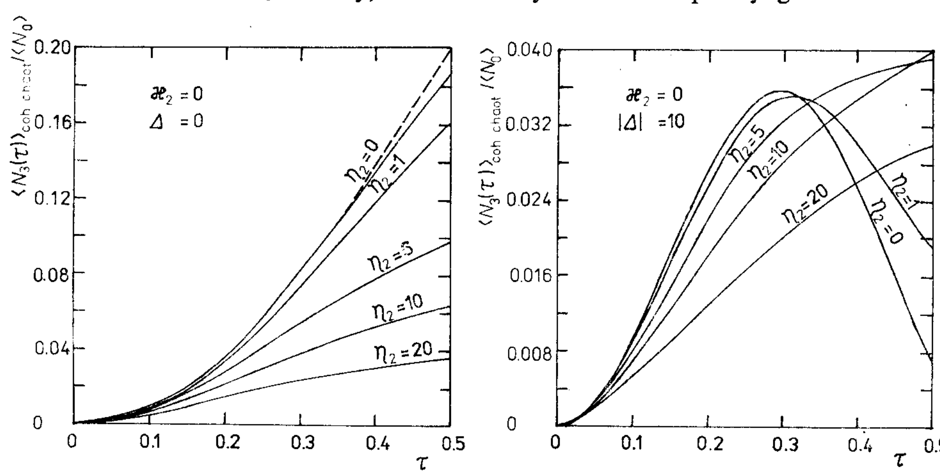

Fig. 1. Evolution of the relative mean photon flux of sum-frequency radiation $\langle N_3(\tau)\rangle_{\text{coh chaot}}$: $\langle N_0\rangle$ ($\langle N_0\rangle = \langle N_{1,0}\rangle = \langle N_{2,0}\rangle$, $\tau = \langle N_0\rangle^{1/2} \mu z$) in the incoherent sum-frequency generation with one coherent and the other chaotic sub-frequency input radiations for the ratio of typical dispersion coefficients $|\varkappa_2| = |\varepsilon_{21}|/|\varepsilon_{23}| = 0$, for perfect phase matching ($\Delta = 0$ — a) and great phase mismatch ($|\Delta| = |\Delta k|/\langle N_0\rangle^{1/2} \mu = 10$ — b), and for several values of the reduced spectral half width of chaotic input radiation $\eta_2 = \Gamma_{2,0}|\varepsilon_{23}|/\langle N_0\rangle^{1/2} \mu$. The dashed line in fig. a) represents the exact solution for coherent interaction ($\Delta = 0$, $\eta_2 = 0$) with coherent and chaotic input radiations after [6].

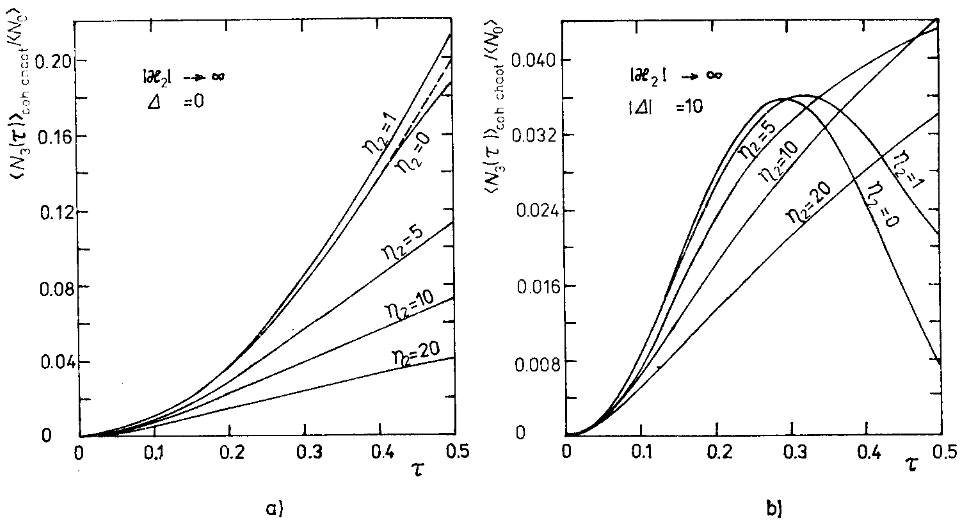

Fig. 2. The same as in fig. 1 for $|\varkappa_2| \to \infty$.

decreases, but later on increases with increasing η_2 in the advancing process (see fig. 1b).

b) Type of interaction: $\gamma^{(I)}_{\omega_1} + \gamma^{(II)}_{\omega_2} \to \gamma^{(I)}_{\omega_3}$ or $\gamma^{(II)}_{\omega_1} + \gamma^{(I)}_{\omega_2} \to \gamma^{(I)}_{\omega_3}$, $\varkappa_2 \approx 2$.

(II.9)
$$\langle N_3(\tau)\rangle_{coh\,chaot} = \langle N_{1,0}\rangle^{1/2} \langle N_{2,0}\rangle^{1/2} \mathscr{I}(\eta_2, \Delta, \tau) - \\ - \langle N_{1,0}\rangle \mathscr{E}_1^{(c,ch)}(\eta_2, \Delta, \tau) - \langle N_{2,0}\rangle \left[\mathscr{E}_2^{(c,ch)}(\eta_2, \Delta, \tau) + \mathscr{F}_1^{(c,ch)}(\eta_2, \Delta, \tau)\right].$$

Our computations have shown that the behaviour of $\langle N_3(\tau)\rangle_{coh\,chaot}/\langle N_0\rangle$ is rather similar to that for $|\varkappa_2| \ll 1$ in this case (see fig. 1). Only the efficiency of sum-frequency generation is somewhat enhanced compared to the previous case. We do not introduce special figures for this case.

2. One sub-frequency is very large in comparison with the other one. Arbitrary type of interaction.

a) $\omega_1 \gg \omega_2$,

$\varkappa_2 \approx 1$.

(II.10)
$$\langle N_3(\tau)\rangle_{coh\,chaot} = \langle N_{1,0}\rangle^{1/2} \langle N_{2,0}\rangle^{1/2} \mathscr{I}(\eta_2, \Delta, \tau) - \\ - \langle N_{1,0}\rangle \mathscr{E}_1^{(c,ch)}(\eta_2, \Delta, \tau) - 2\langle N_{2,0}\rangle \mathscr{E}_2^{(c,ch)}(\eta_2, \Delta, \tau).$$

Similarly as in the previous case ($\varkappa_2 \approx 2$), the course of $\langle N_3(\tau)\rangle_{coh\,chaot}/\langle N_0\rangle$ does not differ much from that for $|\varkappa_2| \ll 1$ (see fig. 1). Computations of equation (II.10) show that for perfect phase matching the course of $\langle N_3(\tau)\rangle_{coh\,chaot}/\langle N_0\rangle$ is an intermediate one between those for $|\varkappa_2| \ll 1$ and $\varkappa_2 \approx 2$, and for great phase mismatch the evolution of $\langle N_3(\tau)\rangle_{coh\,chaot}/\langle N_0\rangle$ is nearly the same as for $\varkappa_2 \approx 2$, for all η_2.

Special figures for this case are not introduced either.

b) $\omega_1 \ll \omega_2$,

$|\varkappa_2| \gg 1$.

(II.11) $$\langle N_3(\tau)\rangle_{\mathrm{coh\,chaot}} = \langle N_{1,0}\rangle^{1/2} \langle N_{2,0}\rangle^{1/2} \mathscr{I}(\eta_2, \Delta, \tau) - $$
$$- \langle N_{1,0}\rangle \mathscr{E}_1^{(c,ch)}(\eta_2, \Delta, \tau) - \langle N_{2,0}\rangle \left[\mathscr{E}_2^{(c,ch)}(\eta_2, \Delta, \tau) + \mathscr{F}_2^{(c,ch)}(\eta_2, \Delta, \tau)\right].$$

The behaviour of $\langle N_3(\tau)\rangle_{\mathrm{coh\,chaot}}/\langle N_0\rangle$ is shown in fig. 2. An interesting effect appears for perfect phase matching and small values of $\eta_2(\eta_2 \lesssim 1)$ (see fig. 2a), namely, the efficiency of the process exceeds that for coherent interaction in this case. For greater values of η_2 and perfect phase matching, as well as for great phase mismatch, the behaviour of $\langle N_3(\tau)\rangle_{\mathrm{coh\,chaot}}/\langle N_0\rangle$ is qualitatively similar as in the previous cases. However, the efficiency of sum-frequency generation is conspicuously enhanced in advancing process compared to that for small $|\varkappa_2|$ (compare figs. 1 and 2).

In order to get better insight into the dependence of the efficiency of sum-frequency generation on the reduced spectral half width η_2 and the ratio of typical dispersion coefficients $\varkappa_2$ (the difference between the group velocities of generating sub-frequency waves), we have plotted the relative mean photon flux $\langle N_3\rangle_{\mathrm{coh\,chaot}}/\langle N_0\rangle$ versus parameter $|\varkappa_2|$ for several values of η_2 in fig. 3, and versus parameter η_2

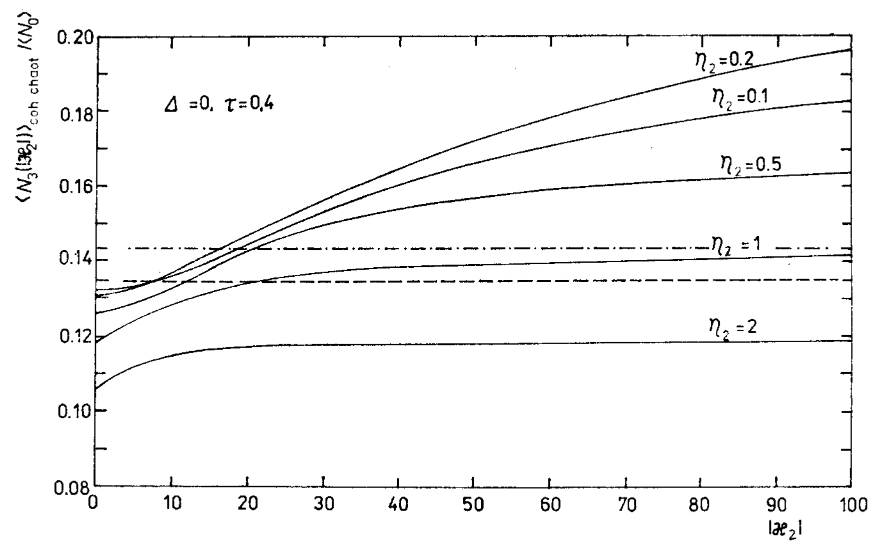

Fig. 3. Relative mean photon flux of sum-frequency radiation $\langle N_3(|\varkappa_2|\rangle_{\mathrm{coh\,chaot}}/\langle N_0\rangle$ versus ratio of typical dispersion coefficients $|\varkappa_2|$ at normalized distance from the nonlinear medium boundary $\tau = 0{\cdot}4$ in the phase matched ($\Delta = 0$) incoherent nonlinear optical interaction for several values of the reduced spectral half width of chaotic input radiation η_2. The dashed line marks the value of $\langle N_3(\tau = 0{\cdot}4)\rangle_{\mathrm{coh\,chaot}}/\langle N_0\rangle$ for coherent ($\eta_2 = 0$) sum-frequency generation with one coherent and the other chaotic input radiations and the dot-dashed line stands for the interaction of coherent radiations.

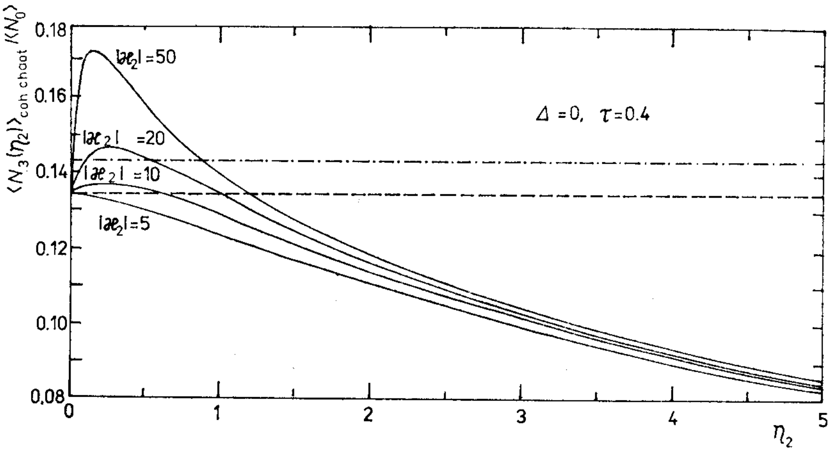

Fig. 4. Relative mean photon flux of sum-frequency radiation $\langle N_3(\eta_2)\rangle_{coh\,chaot}/\langle N_0\rangle$ versus the reduced spectral half width of chaotic input radiation η_2 at the normalized distance from the nonlinear medium boundary $\tau = 0{\cdot}4$ in the phase matched ($\Delta = 0$) incoherent nonlinear optical interaction, for several values of the ratio of typical dispersion coefficients $|\varkappa_2|$. The dashed line marks the value of $\langle N_3(\tau = 0{\cdot}4)\rangle_{coh\,chaot}/\langle N_0\rangle$ for coherent ($\eta_2 = 0$) sum-frequency generation with one coherent and the other chaotic input radiations and the dot-dashed line stands for the interaction of coherent radiations.

for several values of $|\varkappa_2|$ in fig. 4, at normalized distance from the nonlinear medium boundary $\tau = 0{\cdot}4$, for the phase matched process. It is obvious from figs. 3 and 4 that the efficiency of incoherent sum-frequency generation with one coherent and

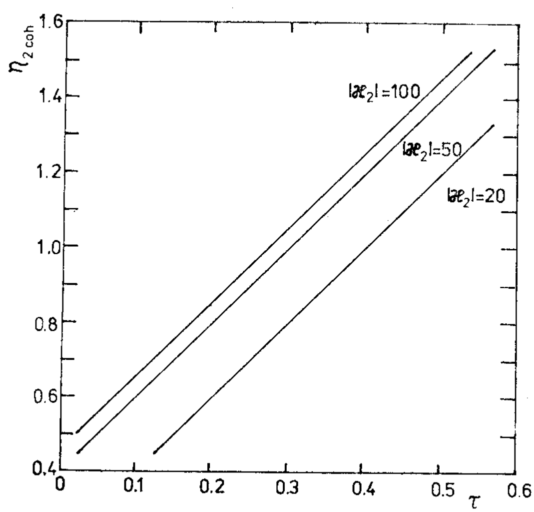

Fig. 5. Ultimate reduced spectral half width of chaotic input radiation η_{2coh}, for which the effect of incoherent sum-frequency generation efficiency enhancement disappears, versus the reduced normal thickness of nonlinear medium τ, for three different values of $|\varkappa_2|$.

the other chaotic input radiations can be enhanced compared to the coherent interaction with one coherent and the other chaotic input radiations, and even it can exceed the efficiency of sum-frequency generation with both coherent sub-frequency input radiations, for small η_2 and great $|\varkappa_2|$. This effect has already been noticed in [9]. A considerable enhancement of the efficiency can be reached for very great values of $|\varkappa_2|$ only. The values of $\eta_{2\max}$, for which the maximum efficiency enhancement occurs, as well as the ultimate values $\eta_{2\mathrm{coh}}$, for which the effect of efficiency enhancement disappears, are dependent on $|\varkappa_2|$ (see fig. 4) and they vary with the normal thickness of nonlinear medium. For illustration we have plotted the ultimate reduced spectral half width $\eta_{2\mathrm{coh}}$ versus the reduced normal thickness of nonlinear medium τ for three different values of $|\varkappa_2|$ in fig. 5. It follows from fig. 5. that $\eta_{2\mathrm{coh}}$ increases linearly with increasing τ for all $|\varkappa_2|$ in the initial stage of the process.

Generally, for small values of the coefficient η_2 (small spectral half width of chaotic input radiation $\Gamma_{2,0}$ and small typical dispersion coefficient $|\varepsilon_{23}|$) the process of incoherent sum-frequency generation is rather sensitive to the reduced phase mismatch $|\Delta|$ and the difference between the group velocities of generating radiations characterized here by $|\varkappa_2|$, and a marked angular or frequency cutoff appears. On the other hand, for greater values of η_2 the process is less sensitive to $|\Delta|$ and $|\varkappa_2|$ and, consequently, broad-angular or broad-band beams of chaotic sub-frequency radiation can be converted with approximately the same, even if low, efficiency.

4. SPECTRAL DISTRIBUTION OF GENERATED SUM-FREQUENCY RADIATION

The spectral distribution of sum-frequency radiation at $\omega_3 = \omega_1 + \omega_2$, generated in the incoherent nonlinear optical interaction with one coherent (ω_1) and the other chaotic (ω_2) input radiations, has been found in the first approximation of the iterative solution to be (see equation (I.30) in [1])

$$g_{3\mathrm{coh\,chaot}}(\Omega, \tau) = \frac{|\varepsilon_{23}|}{\langle N_{1,0}\rangle^{1/4} \langle N_{2,0}\rangle^{1/4} \mu} f_{\mathrm{coh\,chaot}}(\Omega, \tau) , \tag{II.12}$$

where

$$\Omega = \frac{\varepsilon_{23}}{\langle N_{1,0}\rangle^{1/4} \langle N_{2,0}\rangle^{1/4} \mu} (\omega - \omega_{3,0}) \tag{II.13}$$

and

$$f_{\mathrm{coh\,chaot}}(\Omega, \tau) = \frac{\eta_2 \tau^2}{\pi \mathscr{I}(\eta_2, \Delta, \tau)(\eta_2^2 + \Omega^2)} \left\{\frac{\sin[(\Delta + \Omega)\tau/2]}{(\Delta + \Omega)\tau/2}\right\}^2 , \tag{II.14}$$

$\mathscr{I}(\eta_2, \Delta, \tau)$ being given by equation (II.1) and $\omega_{3,0} = \omega_1 + \omega_{2,0}$, where $\omega_{2,0}$ is the mean frequency of chaotic input radiation with Lorentzian spectral distribution, $g_{2,0\mathrm{chaot}}(\omega) = \Gamma_{2,0}/\pi[\Gamma^2_{2,0} - (\omega - \omega_{2,0})^2]$ (see e.g. [10]).

The expression for $g_{3\mathrm{coh\,chaot}}(\Omega, \tau)$ can be simplified in some special cases.

1. For perfect phase matching ($\Delta = 0$) we obtain

$$(II.15) \quad g_{3\mathrm{coh\,chaot}}(\Omega, \tau) = \frac{2|\varepsilon_{23}|\,\eta_2^2 \sin^2(\Omega\tau/2)}{\pi\langle N_{1,0}\rangle^{1/4}\langle N_{2,0}\rangle^{1/4}\mu(\eta_2^2 + \Omega^2)\,\Omega^2\{\tau - (1/\eta_2)[1 - \exp(-\eta_2\tau)]\}}.$$

a) In the case of $\eta_2\tau \ll 1$, i.e. for a high degree if coherence in the chaotic input radiation or for a small dispersion of the medium, or at the beginning of the process, equation (II.15) is reduced to

$$(II.15a) \quad g_{3\mathrm{coh\,chaot}}(\Omega, \tau) = \frac{|\varepsilon_{23}|\,\eta_2}{\pi\langle N_{1,0}\rangle^{1/4}\langle N_{2,0}\rangle^{1/4}\mu(\eta_2^2 + \Omega^2)}\left[\frac{\sin(\Omega\tau/2)}{\Omega\tau/2}\right]^2$$

and in the original variables

$$(II.15a') \quad g_{3\mathrm{coh\,chaot}}(\omega, z) = \frac{\Gamma_{2,0}}{\pi[\Gamma_{2,0}^2 + (\omega - \omega_{3,0})^2]}\left\{\frac{\sin[\varepsilon_{23}(\omega - \omega_{3,0})\,z/2]}{\varepsilon_{23}(\omega - \omega_{3,0})\,z/2}\right\}^2.$$

For a dispersionless medium ($\varepsilon_{23} \to 0$, $\Gamma_{2,0} \neq 0$) equation (II.15a′) provides the Lorentzian spectral distribution, $g_{3\mathrm{coh\,chaot}}(\omega) = \Gamma_{2,0}/\pi[\Gamma_{2,0}^2 - (\omega - \omega_{3,0})^2]$, and for the second-order coherent input radiation ($\varepsilon_{23} \neq 0$, $\Gamma_{2,0} \to 0$) we have $g_{3\mathrm{coh\,chaot}}(\omega) \to \delta(\omega - \omega_{3,0})$. Thus the generated sum-frequency radiation simply copies the spectral distribution of the chaotic sub-frequency radiation in this case.

b) In the case when $\eta_2\tau \gg 1$, i.e. for a small degree of coherence of the chaotic input radiation and great dispersion of the medium, and also for greater values of τ, we have from equations (II.12) and (II.14)

$$(II.15b) \quad g_{3\mathrm{coh\,chaot}}(\Omega, \tau) = \frac{|\varepsilon_{23}|\,\eta_2^2}{2\pi\langle N_{1,0}\rangle^{1/4}\langle N_{2,0}\rangle^{1/4}\mu(\eta_2^2 + \Omega^2)}\left[\frac{\sin(\Omega\tau/2)}{\Omega\tau/2}\right]^2\tau.$$

It follows from equation (II.15b) that the central maximum of sum-frequency radiation becomes narrower with respect to the spectral distribution of the chaotic input radiation and side maxima with decreasing intensity appear at $\Omega = \pm 3\pi/\tau, \pm 5\pi/\tau, \ldots$

2. For considerable phase mismatch ($|\Delta| \gtrsim 1$) the following cases are discussed.

a) If $\eta_2\tau \ll 1$ we have for the spectral density of sum-frequency radiation

$$(II.16) \quad g_{3\mathrm{coh\,chaot}}(\Omega, \tau) = \frac{|\varepsilon_{23}|\,\eta_2}{\pi\langle N_{1,0}\rangle^{1/4}\langle N_{2,0}\rangle^{1/4}\mu(\eta_2^2 + \Omega^2)}\left\{\frac{\dfrac{\sin[(\Delta + \Omega)\,\tau/2]}{(\Delta + \Omega)\,\tau/2}}{\dfrac{\sin(\Delta\tau/2)}{\Delta\tau/2}}\right\}^2.$$

The discussion of equation (II.16) is similar to that for equation (II.15a). The generated sum-frequency radiation approximately copies the spectral distribution of the chaotic input radiation. However, the spectral density $g_{3\mathrm{coh\,chaot}}(\Omega)$ is slightly asymmetric in this case.

b) For $\eta_2 \tau \gg 1$ equation (12) is simplified to

$$\text{(II.17)} \quad g_{3\,\text{coh chaot}}(\Omega, \tau) = \frac{|\varepsilon_{23}| \, (\Delta^2 + \eta_2^2)}{2\pi \langle N_{1,0} \rangle^{1/4} \langle N_{2,0} \rangle^{1/4} \mu (\eta_2^2 + \Omega^2)} \left\{ \frac{\sin [(\Delta + \Omega) \tau/2]}{(\Delta + \Omega) \tau/2} \right\}^2 \tau \, .$$

The spectral distribution of generated sum-frequency radiation is conspicuously asymmetric in this case and its maximum is shifted towards positive or negative values of Ω according to the sign of the phase mismatch Δ.

Fig. 6 shows the spectral distribution function $f_{\text{coh chaot}}(\Omega)$ at two different distances from the nonlinear medium boundary τ and for three values of Δ and two values of η_2. The evolution of spectral half width of the generated sum-frequency radiation was shown in [7].

From fig. 6 it is seen that, generally, there is a tendency to narrowing the spectral width of the generated sum-frequency radiation in the course of sum-frequency generation process.

Moreower, if the phase mismatch is not equal to zero, there is a shift of the central maximum of generated sum-frequency radiation in the following sense. For $\text{sgn}(\Delta k) = \text{sgn}(\varepsilon_{23})$ the central maximum is shifted towards the lower frequencies and a red shift occurs. For $\text{sgn}(\Delta k) = -\text{sgn}(\varepsilon_{23})$ the central maximum is shifted towards the higher frequencies and a blue shift occurs.

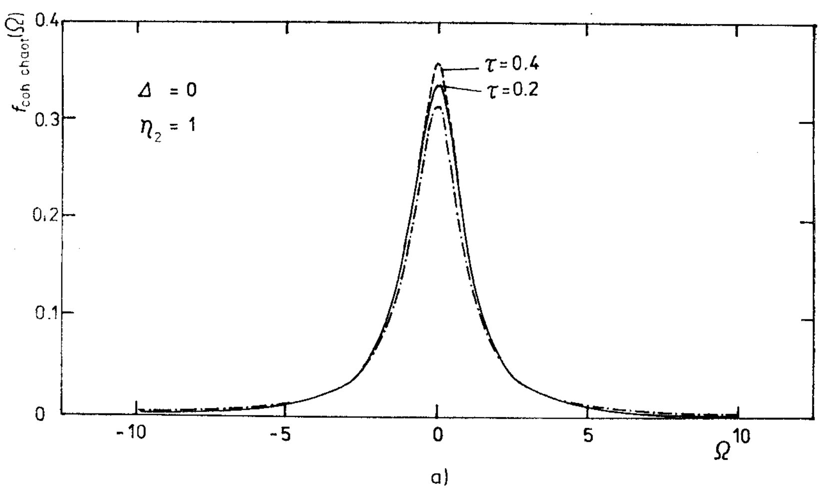

Fig. 6. Reduced spectral distribution of generated sum-frequency radiation $f_{\text{coh chaot}}(\Omega)$ ($\Omega = \varepsilon_{23}(\omega - \omega_{3,0})/\langle N_{1,0} \rangle^{1/4} \langle N_{2,0} \rangle^{1/4} \mu$) for three different values of the reduced phase mismatch $\Delta = \Delta k / \langle N_{1,0} \rangle^{1/4} \langle N_{2,0} \rangle^{1/4} \mu$ and two values of the reduced spectral half width of chaotic input radiation $\eta_2 = \Gamma_{2,0} |\varepsilon_{23}| / \langle N_{1,0} \rangle^{1/4} \langle N_{2,0} \rangle^{1/4} \mu$ at two reduced normal distances from the nonlinear medium boundary $\tau = \langle N_{1,0} \rangle^{1/4} \langle N_{2,0} \rangle^{1/4} \mu z$ in the incoherent sum-frequency generation. The dot-dashed lines represent the spectral distribution of the chaotic input radiation $f_{2,0}(\Omega)$ ($\Omega = \varepsilon_{23}(\omega - \omega_{2,0})/\langle N_{1,0} \rangle^{1/4} \langle N_{2,0} \rangle^{1/4} \mu$). For negative values of Δ the corresponding curves are symmetric with respect to those given above, with $\Omega = 0$.

(continued)

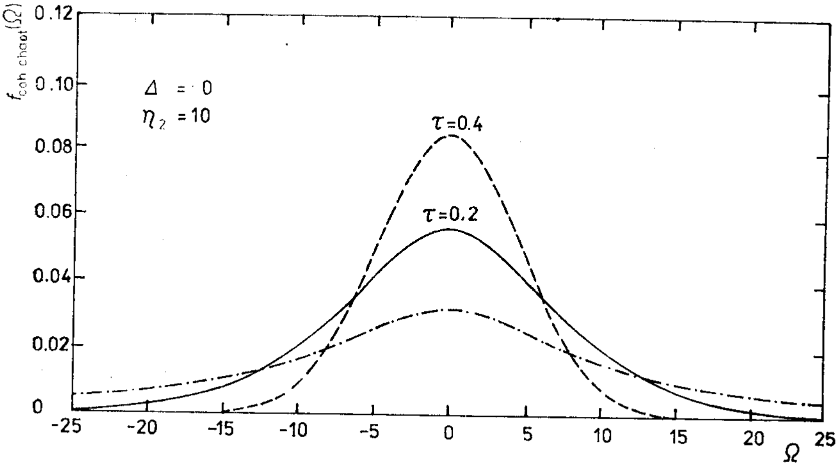
$f_{coh\ chaot}(\Omega)$
Δ = 0
η_2 = 10
τ=0.4
τ=0.2
0.12
0.10
0.08
0.06
0.04
0.02
0
-25
-20
-15
-10
-5
0
5
10
15
20
25
Ω

b)

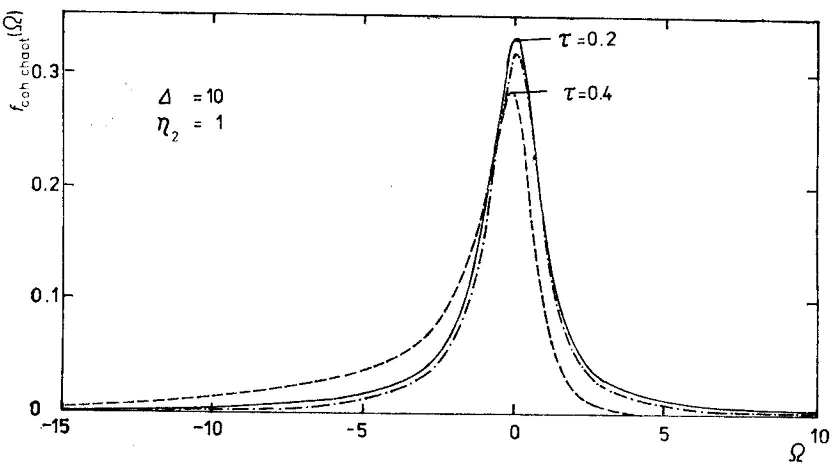
$f_{coh\ chaot}(\Omega)$
Δ = 10
η_2 = 1
τ = 0.2
τ = 0.4
0.3
0.2
0.1
0
-15
-10
-5
0
5
10
Ω

c)

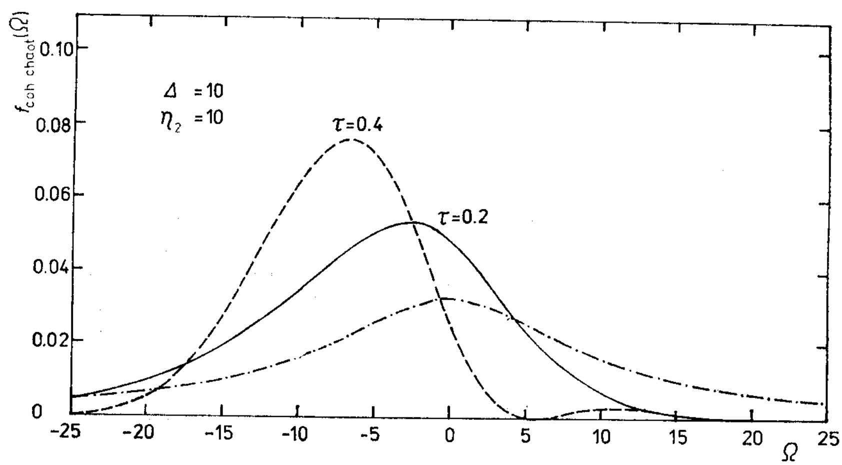
$f_{coh\ chaot}(\Omega)$
Δ = 10
η_2 = 10
τ=0.4
τ=0.2
0.10
0.08
0.06
0.04
0.02
0
-25
-20
-15
-10
-5
0
5
10
15
20
25
Ω

d)

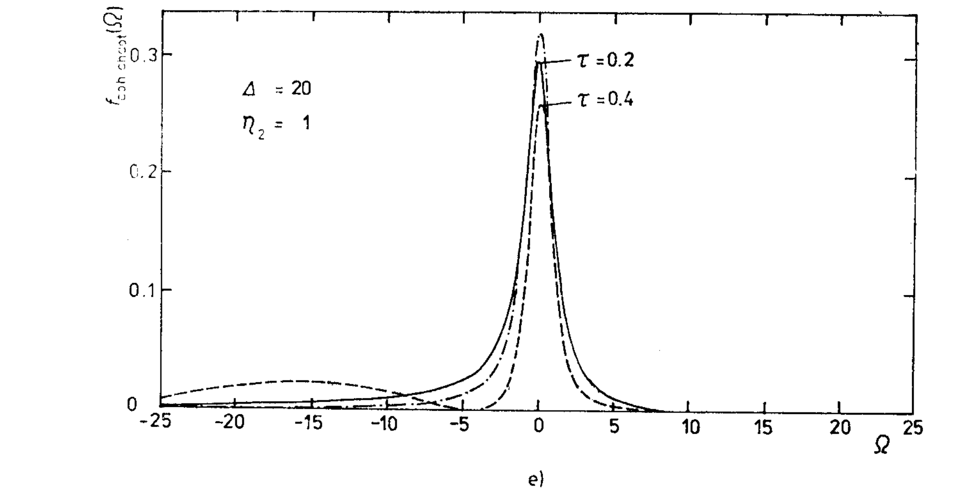

Fig. 6 *(continued)*.

5. DISCUSSION

The above described behaviour of incoherent sum-frequency generation with one coherent and the other chaotic sub-frequency input radiation can be discussed in connection with the fulfilment of phase matching condition, the coherence phenomena, the evolution of light statistics of interacting radiations in the course of nonlinear interaction and the dispersion of nonlinear medium.

It has been shown that for the phase matching or for small phase mismatch ($|\Delta| \ll 1$) and small values of $\eta_2(\eta_2 < \eta_{2\mathrm{coh}})$ the efficiency of incoherent sum-frequency generation increases with increasing $|\varkappa_2|$ and it can exceed that for coherent interaction (see figs. 3 and 4). This enhancement of efficiency of the process can be explained within the framework of light statistics. In [8] it has been shown that during the coherent ($\Delta = 0$, $\eta_2 = 0$) sum-frequency generation with one coherent and the other chaotic sub-frequency input radiations the anticorrelation is generated between sub-frequency radiations. This effect leads to a decrease of efficiency of the process with respect to the interaction of coherent radiations. If there is a difference between the group velocities of sub-frequency waves ($\varkappa_2 \neq 0$) in the nonlinear medium, the generating radiations become spatially (time) shifted, so that the generated anticorrelation is compressed or it can be converted into the correlation between sub-frequency radiations. This gives an increase of the efficiency of sum-frequency generation. However, if the reduced spectral halfwidth of the chaotic sub-frequency input radiation is considerable ($\eta_2 > \eta_{2\text{coh}}$), the efficiency of the process decreases with increasing η_2 (see fig. 4). This is firstly a consequence of the phase mismatch effect. In fact, the phase matching can be exactly adjusted for the central maximum frequences $\omega_{2,0}$ and $\omega_{3,0}$ only, for which the phase matching $\mathbf{k}_{\omega_{3,0}} - \mathbf{k}_{\omega_1} - \mathbf{k}_{\omega_{2,0}} = 0$ is satisfied. If the spectral distribution in the sub-frequency radiation at ω_2 (and consequently also in the sum-frequency radiation at ω_3) is considerably extensive, only relatively small intervals of the frequencies at ω_2 and ω_3 satisfy the approximate phase matching condition for the effective sum-frequency generation: $(\mathbf{k}_{\omega_{3,0}\pm\Delta\omega} - \mathbf{k}_{\omega_1} - \mathbf{k}_{\omega_{2,0}\pm\Delta\omega})_z\, z \lessapprox \pi$ (see e.g. [2, 4]). The remaining satellite frequencies are phase mismatched, meaning that a considerable amount of the sub-frequency radiation energy is converted into the sum-frequency radiation energy with a variously small efficiency and spatial period according to the frequency difference $\Delta\omega = |\omega_{2,0} - \omega_2|$. However, for greater $\eta_2 (\eta_2 > \eta_{2\text{coh}})$ the effect of spatial incoherency of the chaotic sub-frequency and sum-frequency radiations, which prevents the further stimulation of the nonlinear process by the sum-frequency radiation that is generated at former phases of the process, is manifested in the advancing sum-frequency generation [7].

Of course, both the favourable group-velocity dispersion effect and the quenching effects of phase mismatch and spatial incoherency manifest themselves simultaneously. The ultimate value $\eta_{2\text{coh}}$ represents the situation at which these effects cancel out mutually. For $\eta_2 < \eta_{2\text{coh}}$, the accelerating group-velocity dispersion effect predominates over the damping phase mismatch and spatial incoherency effects, and vice versa for $\eta_2 > \eta_{2\text{coh}}$.

The narrowing of the spectral distribution of generated sum-frequency radiation in the course of nonlinear process, which is demonstrated in figs. 6a and 6b, is due to the phase mismatch that limits the effective conversion of satellite frequencies of the chaotic sub-frequency radiation. As the spectral distribution of sum-frequency radiation was described in the first approximation of the iterative solution only, the light statistical (group-velocity mismatch) effects are not included in our description in this case.

In the case of considerable phase mismatch ($|\Delta| \gg 1$) the efficiency of sum-frequency generation first decreases, but later on increases with increasing η_2 in the advancing process (see figs. 1b and 2b), and it is very little dependent on $\varkappa_2$. This is predominantly a consequence of the phase matching effect. At the beginning of the process the phase mismatch does not markedly affect the nonlinear process and the frequency maximum of generated sum-frequency radiation appears at $\omega_{3,0} = \omega_1 + \omega_{2,0}$. However, in the further course of sum-frequency generation a narrow band of sum-frequencies around the frequency $\omega_{3\,\max}$,

$$\omega_{3\,\max} = \omega_{3,0} - \frac{c\,\Delta k \cos \beta_3}{n_{rg3} - n_{rg2} \cos \alpha_{23}}, \tag{II.18}$$

is systematically amplified [7], n_{rgj} being group indices of refraction in ray directions and c is the velocity of light in vacuum. Taking into account the definition of group index (group velocity) [6], it is easy to see that equation (II.18) represents merely the selection rule for such combination of sub-frequency $\omega_{2\,\max} = \omega_{2,0} \pm \Delta\omega_{\max}$ and sum-frequency $\omega_{3\,\max} = \omega_{3,0} \pm \Delta\omega_{\max}$ that satisfies the phase matching condition, $\boldsymbol{k}_{\omega_{3\max}} - \boldsymbol{k}_{\omega_1} - \boldsymbol{k}_{\omega_{2\max}} = 0$. The frequencies which do not satisfy the approximate phase matching condition, $(\boldsymbol{k}_{\omega_3} - \boldsymbol{k}_{\omega_1} - \boldsymbol{k}_{\omega_2})_z\, z \lessgtr \pi$, are damped due to the phase mismatch effect, which is a consequence of destructive interference of radiations that are generated at different distances from the nonlinear medium boundary. The broader is the frequency band (spectral halfwidth $\Gamma_{2,0}$) of chaotic input radiations, the more relative energy belongs to the frequency band which can be effectively converted.

The above described mechanism explains also the shift of the central maximum of resulting radiation in the course of sum-frequency generation for considerable phase mismatch (see figs. 6c, 6d and 6f). In the advancing process the broadening or doubling of the central maximum of sum-frequency radiation can appear (see figs. 6d, 6e and 6f and also [7]), which represents a transient phenomenon only. This is a consequence of competition of the frequency maximum at $\omega_{3,0}$, generated at the beginning of the process, and the later established maximum at $\omega_{3\,\max}$. In the further course of sum-frequency generation the only one conspicuous maximum at $\omega_{3\,\max}$ is assumed to be stabilized. Of course, inasmuch as our discussion is based on the first-step approximate solution only, other phenomena, like the influence of light statistics of interacting radiations and group-velocity dispersion, can be expected in the far advanced sum-frequency generation process as well.

The statistical properties of generated sum-frequency radiation were not considered here because their mathematical treatment is really too much exacting. We expect that in the case, if the efficiency of incoherent sum-frequency generation is enhanced due to the difference between group velocities of sub-frequency waves, the fluctuation level in generated sum-frequency radiation exceeds that for coherent interaction [8], inasmuch as the sum-frequency radiation is preferably generated in the spatial (temporal) regions with greater instantaneous intensities (photon clusters) of the initially chaotic sub-frequency radiation, and the spatial (temporal) shift of sub-frequency radiations enables the continuation of this tendency in the advancing process. This leads to an increase of the instantaneous intensities in the photon-cluster regions of sum-frequency radiation and, consequently, to an enhancement of the chaos in generated radiation.

Received 19 April 1988

References

[1] Chmela P., Ficek Z., Kielich S.: Czech. J. Phys. B *39* (1989) 509.
[2] Zernike F., Midwinter J. E.: Applied Nonlinear Optics. Wiley, New York, 1973.
[3] Stepanov D. Yu., Shigorin V. D., Shipulo G. P.: Kvantovaya Elektron. (Moskva) *11* (1984) 1957.
[4] Chmela P.: Wprowadzenie do optyki neiliniowej. Państwowe Wydawnictwo Naukowe, Warsaw, 1987.
[5] Szivessy G.: Kristalloptik, Handbuch der Physik, B. XX. Springer, Berlin, 1928.
[6] Sommerfeld A.: Optik. Akademische Verlagsgesellschaft Geest & Portig K.-G., Leipzig, 1959.
[7] Chmela P.: Opt. Quant. Electron. *14* (1982) 425, 433.
[8] Chmela P.: Czech. J. Phys. B *38* (1988) 283.
[9] Chmela P., Ficek Z., Kielich S.: Opt. Commun. *62* (1987) 403.
[10] Loudon R.: The Quantum Theory of Light. Clarendon Press, London, 1981.